Origin of the Electrochemical Potential in Intercalation Electrodes: Experimental Estimation of the Electronic and Ionic Contributions for Na Intercalated into TiS_2

Dino Tonti,[†] Christian Pettenkofer,[†] and Wolfram Jaegermann*[,‡]

Department of Solar Energetics SE6, Hahn-Meitner-Institut, D-14109 Berlin, Germany, and Department of Material Science, Darmstadt University of Technology, Petersenstrasse 23, D-64287 Darmstadt, Germany

Received: June 13, 2004

The use of photoelectron spectroscopy for the evaluation of the electrochemical potentials in intercalation phases is presented. An in situ prepared thin film electrochemical cell has been used to relate electrochemical quantities as the change of electrochemical potential with electronic properties measured in UHV, as well as with the change of the chemical potential of the electrons, which is equivalent to the position of the Fermi level inside the solid. The changes observed in photoemission data with intercalation are compared to galvanostatic experiments obtained in electrochemical setups using the same sample. From a comparison of the results it is possible to estimate the ionic and electronic contribution to the battery voltage. For Na intercalated into TiS_2 the results indicate a contribution of the electronic component to the battery voltage of at least 60%.

Introduction

The layered metal chalcogenides are ideal substrates for fundamental investigations of materials properties using surface science techniques. As it is possible to prepare clean surfaces by cleavage of single crystals, e.g., inside the UHV chamber, the electronic properties have been investigated for a number of fundamental and technological applications.[1] As one example, the intercalation of layered chalcogenides have been subject of such studies.[1,2] As the intercalation reaction of alkali into layered chalcogenides and oxides involves the occupation of originally empty conduction band states a systematic investigation of the electronic structure of intercalation phases and their changes with stoichiometry would contribute to a better understanding of involved processes. Especially, the validity of the rigid band model,[3,4] which assumes changed occupation of otherwise unchanged electron states of the host, may be experimentally controlled. However, so far the UHV experiments rely on the in situ deposition on layered chalcogenide substrates to prepare well-defined samples for rigorous surface analysis. There are also very few studies of electrochemically intercalated or deintercalated electrodes that have been analyzed after emersion and transfer into UHV.[5−10] However, the problems related to remaining contaminations and transfer-related modifications have not been solved in a satisfying way and, therefore, only a limited characterization of the detailed changes in electronic structure seems possible.

We have recently introduced a different procedure to investigate changes in electronic structure with intercalation by surface science techniques.[11] For this purpose an in situ (inside the UHV chamber) prepared thin film device based on TiS_2 on Na β''-alumina has been used and the concentration of the alkali (in this case Na) can be controlled by externally applied electric potentials. We think that the procedure can be applied to a wide range of intercalation materials and will allow us to obtain a detailed analysis of the electronic structure changes with intercalation. We want to present in this contribution a detailed study of the electrochemical potentials in a comparison of UHV measurements using photoelectron spectroscopy and electrochemical measurements of the same samples.

Theoretical Considerations

The intercalation reaction implies the occupancy of empty sites of a solid host material by a guest species according to the reaction

$$xA + MX_2 \rightarrow A_xMX_2 \quad (1)$$

If the guest's occupied states (given by the ionization potential) are above the host's unoccupied states (given by the electron affinity), as for the intercalation of alkali into the layered chalcogenides, an electron transfer is expected from the guest to the host; therefore, reaction 1 is considered to be a topotactic redox reaction.[12] This reaction is considered to be the driving force of the spontaneous intercalation of alkali metals in a large number of oxides and chalcogenides.[13,14] Besides the energy gain of the electron transferred to a level of lower energy (larger binding energy), the electrostatic interaction between negatively charged host and guest cation provides a further favorable energy contribution for intercalation. However, this partition may be considered to be artificial as the two effects are not independent. In reality, the cation polarizes the neighboring hosts' anions. The negative charge attracted around the cation will also affect both the ionic interaction and the position of the electronic levels of host and guest. As a complete ionization can also not be expected, a covalent interaction from the hybridization of guest and host electron states will also be present. Thus, for a rigorous calculation of the intercalation energy, the total energy of the intercalated compound must be estimated. Indeed, it is possible even to calculate the electrode potential at a given alkali concentration by using density functional theories.[15−17] However, a conceptual splitting of the energy of intercalation into

* To whom correspondence should be addressed. E-mail: jaegerw@surface.tu-darmstadt.de. Fax: +49-6151-16-6308.
† Hahn-Meitner-Institut.
‡ Darmstadt University of Technology.

10.1021/jp047450o CCC: $27.50
Published on Web 09/22/2004

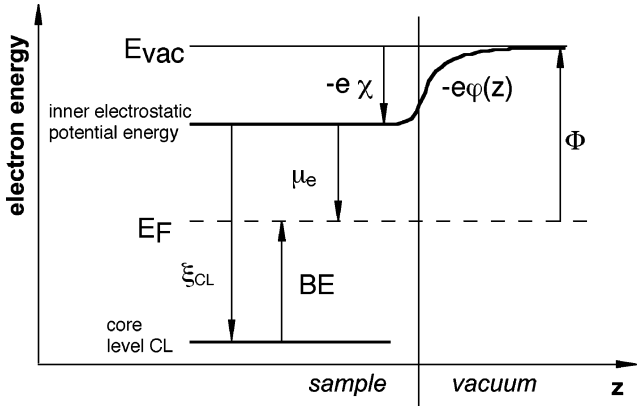

Figure 1. Diagram of the energetic levels inside a solid. Arrows pointing upward express positive values. The profile of the electrostatic potential $\varphi(z)$ is only tentative.

an ionic and an electronic contribution is still useful to understand the nature of energy storage and their dominant contributions, which are helpful for a selection of guest materials.

The process described by eq 1 can be the overall reaction of an electrochemical cell where one electrode is the host (cathode, abbreviated with "c" in the notation hereafter) and the other is the pure guest (anode, "a"). If A is an alkali metal, the electrolyte can be a solid or liquid medium, which is an electron insulator and a conductor of ions A^+. The A electrode will charge negatively due to the tendency to release A^+ in the electrolyte, and the host will charge positively due to the diffusion of A^+ from the electrolyte. The charging of both electrodes creates a barrier to further ion diffusion. If the external circuit is closed, electrons will neutralize the charges and the two half-reactions will proceed spontaneously: the cell will work as a battery during discharge. At open circuit a voltage $V(x)$ will be established, which depends on the chemical potential of the alkali A in both electrodes:[18]

$$-eV(x) = {}_{\mathrm{c}}\mu_{\mathrm{A}}(x) - {}_{\mathrm{a}}\mu_{\mathrm{A}}(x) = \Delta\mu_{\mathrm{A}}(x) \tag{2}$$

Without making any assumption on the state of the guest in the intercalated phase, Gerischer et al.[19] have shown that eq 2 may be rewritten as

$$-eV(x) = \Delta\mu_{\mathrm{A}^+}(x) + \Delta\mu_{\mathrm{e}}(x) \tag{3}$$

This corresponds to the aforementioned conceptual partition of the intercalation energy (equivalent to the difference in chemical potential) into an ionic and an electronic component.

Let us now focus on the host electrode. The chemical potential μ_{e} of the electrons in a solid corresponds to the distance of the Fermi level from the level of the Galvani (inner) potential (Figure 1). A measurable quantity is the work function Φ, which in addition contains the unknown contribution of the surface dipole potential $-e\chi$ (note the difference in sign: work function positive and chemical potential negative).

The chemical potential of the ions depends on their activity in the host

$$\mu_{\mathrm{A}^+} = \mu^0_{\mathrm{A}^+} + kT \ln \frac{a_{\mathrm{A}^+}}{a^0_{\mathrm{A}^+}} \tag{4}$$

and can be related to the site energy. In the course of intercalation changes of the local environment of the ions may be thought to be quite smooth. The chemical potential of the ions can then be considered nearly constant compared to the chemical potential of the electrons if at a particular guest concentration the DOS above the Fermi level is small. On the basis of this assumption some authors could explain the voltage−composition profile of intercalation cells by considering the electronic valence structure of the host, assuming that it does not change upon intercalation (rigid band model).[20−23] On the other hand, in the presence of energetically inequivalent intercalation sites, steps may appear, which can be associated with the variations of the chemical potential of the ions when the more favorable site is no more available. In the case of hosts presenting a mix of different sites and of different electron acceptor levels, it has been possible to distinguish steps corresponding to a transition of the chemical potential either of the ions or of the electrons.[23,24]

An estimation of the chemical potential of the electrons is possible by measurements of the work function Φ, e.g., by photoelectron spectroscopy.[19,25] As mentioned above, the electronic chemical potential μ_{e} corresponds to the difference between the Galvani potential and the Fermi level (Figure 1). The chemical potential of the electrons is thus related to the work function through the relation[26]

$${}_{\mathrm{c}}\mu_{\mathrm{e}} = e\chi - {}_{\mathrm{c}}\Phi \tag{5}$$

containing a surface dipole contribution $e\chi$. If the surface potential can be considered constant, the increase of the work function is equivalent to the decrease of chemical potential. If the battery voltage is also measured, by differentiating and rearranging eq 3, one can extrapolate the ionic contribution according to

$$\frac{\mathrm{d}}{\mathrm{d}x}\,{}_{\mathrm{c}}\mu_{\mathrm{A}^+} = -e\frac{\mathrm{d}}{\mathrm{d}x}V - \frac{\mathrm{d}}{\mathrm{d}x}\,{}_{\mathrm{c}}\mu_{\mathrm{e}} = -e\frac{\mathrm{d}}{\mathrm{d}x}V(x) - \frac{\mathrm{d}}{\mathrm{d}x}\,{}_{\mathrm{c}}\Phi(x) \tag{6}$$

However, it is not possible a priori to establish whether the surface dipole remains constant during intercalation. In addition, the formation of adsorbates cannot be well controlled if ex situ intercalated materials are measured. Intercalation is possible in UHV by deposition of alkali metals,[27−29] but also in this case the formation of adatoms has been proven.[1,30−35] Due to these experimental difficulties only very few attempts have been reported using the work function to evaluate the chemical potential of the electrons.[36,37] In this paper we will present results obtained from the combination of XPS and electrochemical measurements on a solid-state cell to evaluate the relative ionic and electronic contributions to the electrode potential. We propose that a better probe of the chemical potential of the electrons is the binding energy change (BE) of a spectator element, whose chemical shift is not affected by intercalation. Usually, the binding energy (BE) in solids as measured with photoelectron spectroscopy is referred to the position of the Fermi level within the solid. For this purpose we define the internal binding energy (IBE) as the energy distance ξ_{CL} between the energy of the core level lines and the Galvani potential (the vacuum potential inside the phase without the contribution of the surface dipole, see Figure 1). The IBE is referred to the Galvani potential as the BE is to Fermi level. ξ_{CL} is related to the electronic chemical potential and the binding energy of that level in reference to the Fermi level:

$$\xi_{\mathrm{CL}} = \mu_{\mathrm{e}} - \mathrm{BE}_{\mathrm{CL}} \tag{7}$$

The introduction of the inner binding energy is also necessary to separate effects due to the changed position of the Fermi level (the usual reference level in photoemission) resulting from

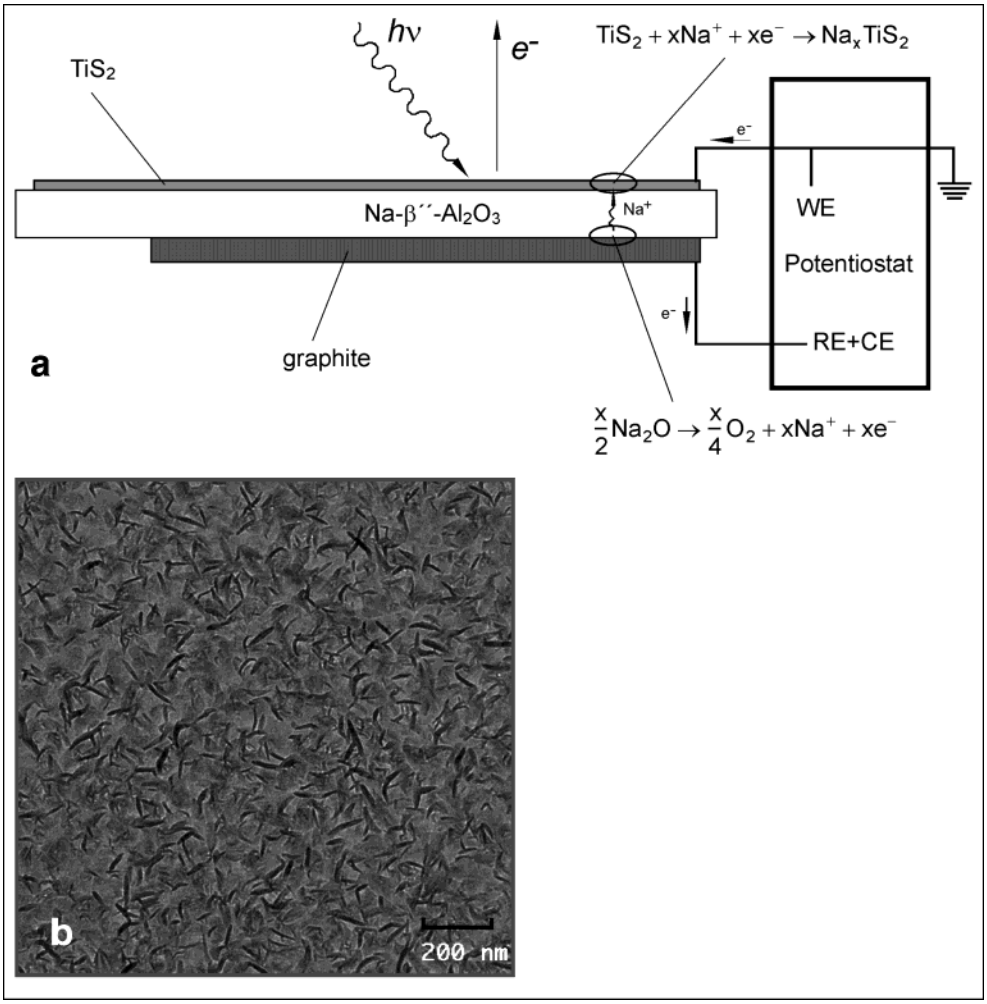

Figure 2. (a) Scheme of the TiS_2/Na-$\beta''$$Al_2O_3$/graphite electrochemical cell mounted for the PES measurements. (b) TEM micrographs of the TiS_2 films used for the experiments.

a changed electron distribution (charge transfer guest−host) from changes of chemical shifts due to changes in electron distribution between the different elements in the solid (different charging of the different elements). As the intercalation will lead to an occupation of previously empty conduction band states, a shift of the Fermi level (equivalent to the position as given by μ_e) is expected. It should be clearly noted at this point that a comparison of BE values of phases before and after intercalation as usually measured in reference to the Fermi level does not allow us to assign different relative charging of host or guest elements (chemical shifts). The Fermi level may be situated at a different level in different intercalation phases and will also change with intercalation; only the internal binding energy ξ_{CL} would allow such comparisons. In addition, binding energy shifts due to charge transfer (initial state) may be compensated by modified screening conditions (final state). The change in binding energy of a spectator element dispersed in the cathode will be a reference for the position of the Fermi level as the potential drop across the surface (modified by adsorbates) will not affect the measurement in contrast to work function determination as given by the secondary cutoff.

Experimental Section

The experiments have been performed in an integrated UHV preparation and analysis system consisting of a Leybold multitechnique photoelectron spectrometer and various home-built deposition chambers connected via UHV transfer chambers. More detailed information of the system may be found elsewhere.[38] Valence band spectra were recorded using He I excitation. All other photoelectron spectra reported here were measured in normal emission using Mg Kα radiation. The binding energy (BE) scale was calibrated to the Au $4f_{7/2}$ and the Cu $2p_{3/2}$ emissions at BE = 84.0 and BE = 932.7 eV, respectively, with BE=0 equivalent to the position of the Fermi level of a Au sample. The work function change with intercalation has been deduced from changes of the secondary electron onset using a bias voltage of −2 V.

We have already described elsewhere in more detail the UHV preparation of a solid-state electrochemical cell suitable for in situ XPS investigations.[11,39] The best results for TiS_2 deposition were using $TiCl_4$ and TBDS (*tert*-butyl disulfide) as metal organic precursors. The core and valence band photoelectron spectra show that stoichiometric TiS_2 films have been prepared. The cell consists of a TiS_2 thin film deposited onto a Na β''-alumina plate. TEM and AFM micrographs showed that the film consists of about 20 nm large platelets oriented perpendicularly to the substrate. The thin film was contacted with a PAR 362 potentiostat as a working electrode. The back of the plate was covered with a graphite layer and used as counter electrode. By controlling the potentiostat voltage, it was possible to reversibly intercalate and deintercalate Na in the TiS_2 thin film. The schematic set up of the experiment is shown in Figure 2. The front contact to the metallic TiS_2 film was a cantilever, electrically isolated to the back contact given by the substrate,

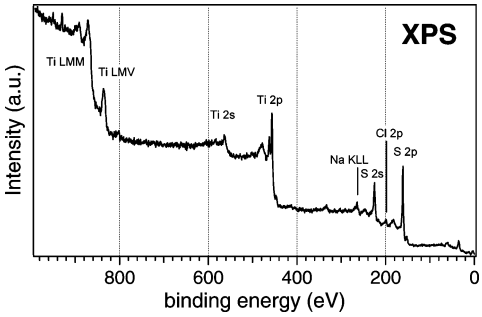

Figure 3. Overview XP spectrum excited with Mg Kα radiation of the TiS_2 thin film deposited on the Na β''-alumina plate after prolonged polarization at a +2.4 V bias.

which was switched to the sample after film preparation using a wobble stick. The morphology of the film as obtained by TEM measurements showing the TiS_2 nanocrystallites is also presented in Figure 3b.

It was not possible to use metallic Na or Na-intercalated graphite as the reference electrode because of the contamination hazard for the vacuum system. Simply a graphite layer was used as the counter electrode. A mass spectrometer could detect the development of O_2 traces in the UHV chamber during the intercalation phases as evidence for the partial decomposition of the alumina. This did not affect significantly the reproducibility of all phenomena observed in the course of many intercalation−deintercalation cycles. The electrochemical reference experiments have been performed in a N_2 filled glovebox using the same specimen as for the UHV experiments. A three-electrode configuration was used, where metallic Na was pressed against the alumina plate to obtain both reference and counter electrodes. The current densities set for the galvanostatic experiments were 1 $\mu A/cm^2$.

Experimental Results

An overview XP spectrum of the deintercalated thin film deposited on the alumina is reported in Figure 3. Besides the substrate signals, a residual Na signal is clearly shown by the Na KLL structure, which is already existent after preparation of the TiS_2 thin films and which does not change considerably after a number of charging/decharging cycles. Also a Cl 2p peak is clearly visible. To calculate stoichiometries, the intensities of the Na 1s (outside the BE range shown in Figure 4) and Cl 2p signals were used, after correction by their ionization cross section (according to the values reported by Yeh and Lindau[40]) and the spectrometer transmission function (after the constructor's specifications). A concentration ratio of nearly 1:1 resulted, indicating the formation of a NaCl impurity phase from a side reaction between the Ti precursor $TiCl_4$ and the Na alumina during film formation. The different chemical nature of this Na species initially present is also evident from its Na KLL Auger line, which is considerably shifted from that of intercalated Na. By comparison with the corrected Ti 2p intensity, the amount of NaCl is about 15% that of TiS_2.

The spectral features of the Na 1s core level emission and the Na KLL emission are shown in Figure 4. The Na 1s signal shows contributions of the contamination phase NaCl, the intercalated Na in TiS_2, and maybe adatoms. These are measured at a BE of about 1073 eV when the film is intercalated, as can be deduced by comparison to adsorption experiments of Na onto TiS_2 single crystals (the spectra are also included in Figure 4). It is interesting to see that also in the experiments reported here, where Na is provided from the backside of the film, part of the transferred Na is also adsorbed on the surface. This fact suggests that there are highly preferential bonding sites available, most probably at edge sites of the crystallites (compare Figure 2b). The results as obtained from the Na KLL lines (Figure 4b) give clearer spectral information. The NaCl signal shows a weak contribution centered at a BE of 264.0 eV when the film is deintercalated. With intercalation (and deintercalation) a signal grows in (and diminishes again) at a BE of 260.8 eV. Again in comparison to the Na adsorption experiments it can clearly be assigned to the intercalated Na. There is no decomposition of the substrate involved in the given charging−discharging range of about Na_xTiS_2, as is clear from the lack of decomposition products in the core level lines of Ti and S and the valence band spectra measured by UPS (a detailed analysis of the changes in electronic structure will be published elsewhere[41]).

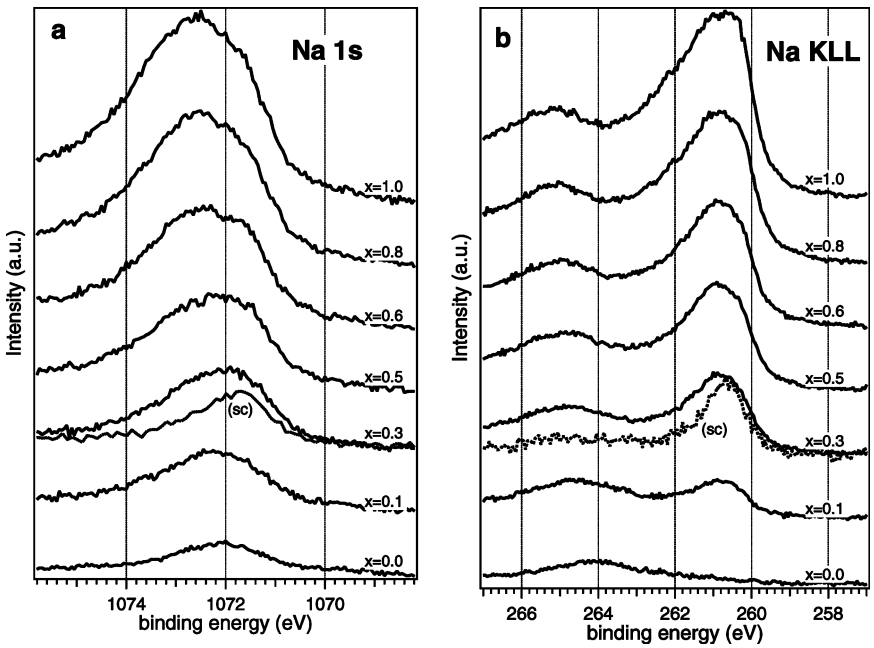

Figure 4. Na 1s XPS (a) and Na KLL Auger (b) signal recorded with Mg Kα excitation energy for the TiS_2 thin film electrochemically intercalated and for a TiS_2 single crystal intercalated by deposition (dashed line, marked with "sc").

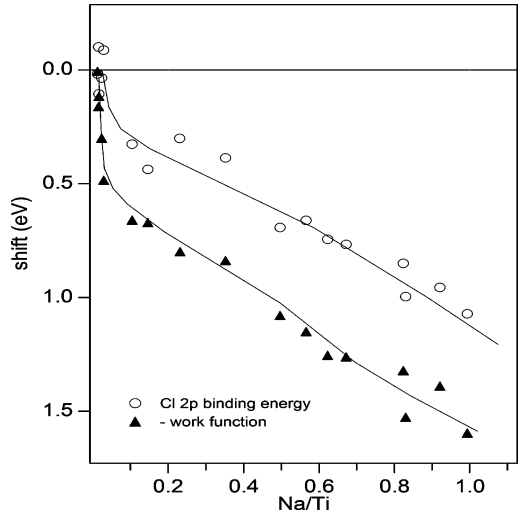

Figure 5. Shifts for the Cl 2p core-level lines and the work function as a function of the intercalated Na amount. The work function was calculated from He I spectra, from the difference between the excitation energy of 21.22 eV and the onset of the secondary background. BEs are based on a one-component fit of the Cl 2p XPS core levels, performed after background subtraction. The variation of work function, with the sign changed for consistency, is also reported. The lines are given as a guide to the eye.

The charge transfer associated with alkali intercalation leads to the filling of empty states in the conducting band, and consequently to a shift of the Fermi level, which implies a change for all binding energies. This change is evaluated in Figure 5, where the shift of the binding energy of the Cl 2p core levels is compared with the variation of the work function. Also, the core level lines of the other elements show a BE shift, which, however, is smaller due to the superposition of different effects (for details see ref 41).

Also shown is the change of the work function as has been deduced from the He I spectra using the edge of the secondary electrons. Due to the weakness of the Cl signal, the BE is affected by a larger error than the work function. The drawn lines represent approximately the mean values for a given Na concentration. It can be well appreciated that for a larger Na concentration the work function has only a slightly higher slope than the Cl 2p binding energy, and both measurements appear to be a good estimation of the variation of the electronic chemical potential. Instead, at low Na concentrations ($x < 0.2$) the variation is steep for both, but different. It is well-known that alkali metals adsorbed on a surface strongly reduce the work function.[42] This is due to the formation of a surface dipole change $\Delta\chi$ consisting of the positive adatom layer and the solids' counter charge. This is frequently observed also on samples intercalated by deposition, if part of the alkali metal remains on the surface.[1,32,35] Often in these cases it has been also possible to recognize the distinct components on the XPS signals of the alkali species, associated with the surface and bulk (intercalated) species. Evidently, even if electrochemically intercalated from the bottom, in this case some Na is present on the surface. The fact that Na was not deposited but spontaneously diffused to the surface from the interior suggests that this state is not metastable, as often inferred when observed with single crystals but thermodynamically favored. A likely explication can be the extreme roughness of the nanocrystalline TiS_2 thin film, which evidently provides highly stable sites for Na in nearly ionic form located at grain boundaries and interstices.

The electrochemical potential of the TiS_2 electrode as a function of the charge has been measured later in the glovebox

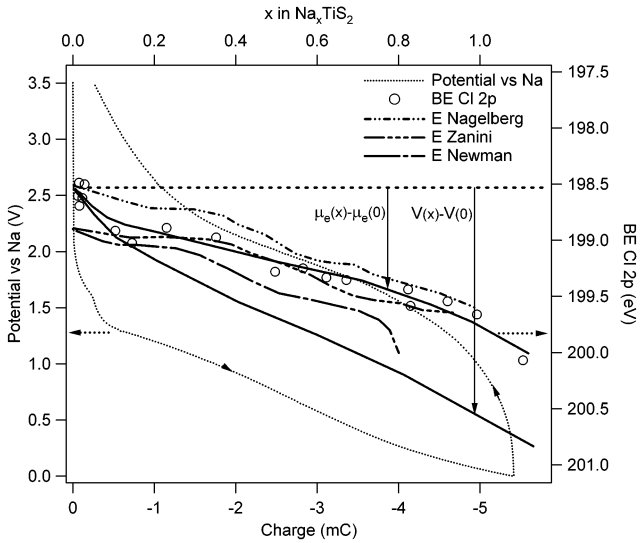

Figure 6. Variation of the electrochemical potential and of the chemical potential of the electrons in a TiS_2 thin film cathode as a function of the intercalated Na content. The electrochemical potential is deduced from the voltage in a three-electrode cell, and the chemical potential of the electrons from the Cl 2p binding energy shift. The lines are given as a guide to the eye and are approximately deduced from the average values of voltage or binding energy. Note that the arrows have the same orientation due to the opposite scale of the left and right axis. For a reference are shown also the potentials reported by other authors.[43,45,46]

on the same cell used in UHV experiments. The voltage vs charge profile for a charge−discharge cycle is reported in Figure 6. Compared with the literature for the electrochemical intercalation of Na into a TiS_2 powder[43−46] the voltage drops to much lower values (up to 1 V less for similar x), and the curve does not exhibit evident steps. The measurement in the literature refers to pellet electrodes made of pressed powder. In our case, both sample thickness and grain size are in a submicrometer scale; therefore, surface effects will play a more dominant role. Additionally, from the occupation of the Ti 3d states in the valence band spectra, we estimate an excess amount of Ti on the order of 10% in the prepared thin film. This excess occupies sites in the van der Waals gap (self-intercalated Ti) and donates electrons to the conduction band of TiS_2, decreasing considerably the free energy of Na intercalation.[13,47,48] It is also clear from the hysteresis of the current−voltage curve that probably due to the high resistivity of the Na β-alumina there is a strong polarization effect in our experiments.

The thick line is taken as a medium level of the potential variations with intercalation as it follows from our experiments. Also shown are mean values of the change of battery voltage as it follows from the literature data. On the same energy scale of the cell voltage the variations of Cl 2p BE are reported, which reflect the change in Fermi level position with intercalation, as will be discussed in detail in the next section.

Discussion

The NaCl contamination phase does not interfere with the intercalation process. Therefore, the chemical environment of Cl is expected to remain unchanged during the intercalation−deintercalation cycles. As a consequence, the inner BE ξ for all Cl electronic levels should keep constant. Possible shifts in the position of the Fermi level (decreasing μ_e) due to the filling of conduction band states with intercalation will lead to an identical increase of the BE as measured with respect to the Fermi level.

By differentiating the expression (7) with the only assumption that the contact potential between TiS_2 and NaCl contamination phases can be considered constant too, we obtain for the Cl 2p core level:

$$\frac{d}{dx}\xi_{Cl2p} = \frac{d}{dx}\mu_e - \frac{d}{dx}BE_{Cl2p} = 0 \quad (8)$$

Therefore, shifts of the BE will just reflect variations of the Fermi level reference, and thus of the electronic chemical potential.

The relations (5) and (7) although independent, have the same form and express the chemical potential of the electrons as the sum of two terms, one that can be directly measured by photoelectron spectroscopy, and one that may be assumed constant. The consistency of these assumptions has already been evaluated in Figure 5, where the shift of Cl BE has been compared to the change of work function. The initial reduction of work function is larger than the increase of the binding energy. Evidently, the formation of a surface dipole makes the work function not very liable for the evaluation of the variation of chemical potential of the electrons. For this reason, we will identify the variation of the electronic chemical potential with the shift of the Cl 2p peak. Therefore, eq 6 will not be considered, but the following:

$$\frac{d}{dx}\mu_{A^+} = -e\frac{d}{dx}V - \frac{d}{dx}BE_{Cl2p} \quad (9)$$

The comparison of the change of battery voltage and the change of Cl BE representing the change of the electrochemical potential of the electrons (excluding surface dipole effects) with intercalation is shown in Figure 6. Our data suggest that the battery voltage is governed by two-thirds by the contribution of the electrochemical potential of the electrons and one-third by that of the ions. As our electrochemical results may be influenced by polarization effects, we have also included in Figure 6 the mean voltage change as reported by several authors.[43,45,46] Compared to these data, the contribution of the electronic part would be higher, approaching nearly 100%. Initially, the rapid fall of the voltage matches the fall of the electronic chemical potential. This is possibly due to the relatively low density of the empty states immediately above the Fermi level. For higher Na contents it can be seen that the voltage decreases more rapidly in our experiments than the line formed by the BE values measured with PES. By considering the different slopes with the proper sign, it must be concluded that the chemical potential of the A^+ ions increases in the TiS_2 electrode when their activity (eq 4) increases. This agrees with the intuition. Therefore, in the investigated system the variation of the voltage may be associated with the increase of chemical potential of not only the electrons, but also of the ions. We cannot exclude, however, that this effect is mostly due to experimental difficulties with our setup.

In addition, we have analyzed the change of the electrochemical potential inside the phase by neglecting surface dipole contributions, assuming them to be a specific problem of the UHV surface science experiments. However, it is known that for some battery materials a solid/electrolyte interface phase (SEI) is formed. A priori one may also assume that such interfaces may contribute to a voltage drop across the phase boundary and reduce the battery voltage. Comparing the experimentally determined voltage drops or our films in Figure 6 with the change of work function, one may conclude on a better resemblance of data. This would imply a double layer potential drop across the phase boundary alumina/TiS_2 (cathode/electrolyte). For analyzing this effect, the comparison of binding energy changes of spectator atoms may be compared to the changes in work function of electrodes transferred from the electrolyte into UHV and to the corresponding battery voltages. We have recently built the equipment that may allow for such experiments, and we want to address this problem in future studies.

Summary and Conclusions

We have presented a new procedure for the experimental study of intercalation reactions using photoelectron spectroscopy on in situ prepared and electrochemically controlled devices. With this technique valuable and so far lacking information can be directly obtained on the changes of electronic structure and on the variations of the electrochemical potentials of electrons with intercalation degree. By comparing electronic changes with the electrode potential the relative contributions of the ionic and electronic contribution to the battery voltage can be estimated. In the case of Na intercalation into TiS_2 at least two-thirds of the battery voltage is due to the electronic part. The rather large contribution of the ionic part is assigned to inefficient screening of the Na ions within the van der Waals gap of the lattice, which may be related to the covalent rather than ionic character of the host compound. Desirable improvements of the experimental procedure include the use of highly ion-conducting solid-state electrolytes, to reduce polarization effects, and of UHV compatible counter electrodes instead of Na in graphite, to allow for a complete electrochemical analysis during the UHV experiments. Finally, a systematic comparison of electrochemical data and related surface properties after emersion using optimized transfer conditions with the type of UHV in situ experiments presented here may provide a deeper insight into the chemical properties and the electronic structure of intercalation phases present in real systems.

References and Notes

(1) Starnberg, H. I. *Mod. Phys. Lett. B* **2000**, *14*, 455.
(2) Jaegermann, W.; Tonti, D. Surface Science Investigations of Intercalation Reactions with Layered Metal Dichalcogenides. In *New Trends in Intercalation Compounds for Energy Storage*; Julien, C., Pereira-Ramos, J. P., Momchilov, A., Eds.; Kluwer: Dordrecht, 2002; Vol. 61, p 289.
(3) Acrivos, J. V.; Salem, J. *Philos. Mag.* **1973**, *30*, 603.
(4) Friend, R. H.; Yoffe, A. D. *Adv. Phys.* **1987**, *36*, 1.
(5) Xia, J.; Aubke, F. *J. Fluorine Chem.* **1992**, *57*, 53.
(6) Soedergren, S.; Siegbahn, H.; Rensmo, H.; Lindstroem, H.; Hagfeldt, A.; Lindquist, S.-E. *J. Phys. Chem. B* **1997**, *101*, 3087.
(7) Aurbach, D.; Markovsky, B.; Weissman, I.; Levi, E.; Ein-Eli, Y. *Electrochim. Acta* **1999**, *45*, 67.
(8) Salvi, A. M.; Decker, F.; Varsano, F.; Speranza, G. *Surf. Interface Anal.* **2001**, *31*, 255.
(9) Talledo, A.; Valdivia, H.; Benndorf, C. *J. Vac. Sci. Technol., A: Vacuum, Surf., Films* **2003**, *21*, 1494.
(10) Coluzza, C.; Cimino, N.; Decker, F.; Di Santo, G.; Liberatore, M.; Zanoni, R.; Bertolo, M.; La Rosa, S. *Phys. Chem. Chem. Phys.* **2003**, *5*, 5489.
(11) Tonti, D.; Pettenkofer, C.; Jaegermann, W. *Electrochem. Solid-State Lett.* **2000**, *3*, 220.
(12) Schoellhorn, R.; Sick, E.; Lerf, A. *Mater. Res. Bull.* **1975**, *10*, 1005.
(13) Whittingham, M. S. *Prog. Solid State Chem.* **1978**, *12*, 41.
(14) Hagenmuller, P. *J. Phys. Chem. Solids* **1998**, *59*, 503.
(15) Ceder, G.; Aydinol, M. K.; Kohan, A. F. *Comput. Mater. Sci.* **1997**, *8*, 161.
(16) Aydinol, M. K.; Kohan, A. F.; Ceder, G. *J. Power Sources* **1997**, *68*, 664.
(17) Benedek, R.; Thackeray, M. M.; Yang, L. H. *J. Power Sources* **1999**, *82*, 487.
(18) McKinnon, W. R.; Haering, R. R. Physical Mechanisms of Intercalation. In *Modern Aspects of electrochemistry*; White, R. E., Bockris, J. O. M., Conway, B. E., Eds.; Plenum Press: New York, 1983; Vol. 15, p 235.

(19) Gerischer, H.; Decker, F.; Scrosati, B. *J. Electrochem. Soc.* **1994**, *141*, 2297.
(20) Dahn, J. R.; Reimers, J. N.; Sleigh, A. K.; Tiedje, T. *Phys. Rev. B* **1992**, *45*, 3773.
(21) Molenda, J.; Bak, T.; Marzec, J. *Phys. Status Solidi A—Appl. Res.* **1996**, *156*, 159.
(22) Gao, Y.; Myrtle, K.; Zhang, M.; Reimers, J. N.; Dahn, J. R. *Phys. Rev. B* **1996**, *54*, 16670.
(23) Obrovac, M. N.; Gao, Y.; Dahn, J. R. *Phys. Rev. B* **1998**, *57*, 5728.
(24) McKinnon, W. R.; Selwyn, L. S. *Phys. Rev. B* **1987**, *35*, 7275.
(25) *Photoemission in Solids*; Cardona, M.; Ley, L., Eds.; Springer: Berlin, 1979.
(26) Lang, N. D.; Kohn, W. *Phys. Rev. B* **1971**, *3*, 1215.
(27) Starnberg, H. I.; Hughes, H. P. *J. Phys. C* **1987**, *20*, 4429.
(28) Ohuchi, F. S.; Jaegermann, W.; Pettenkofer, C.; Parkinson, B. A. *Langmuir* **1989**, *5*, 439.
(29) Weitering, H. H.; Hibma, T. *J. Phys.—Condens. Matter* **1991**, *3*, 8535.
(30) Brauer, H. E.; Ekvall, I.; Olin, H.; Starnberg, H. I.; Wahlstrom, E.; Hughes, H. P.; Strocov, V. N. *Phys. Rev. B* **1997**, *55*, 10022.
(31) Brauer, H. E.; Starnberg, H. I.; Hollenboom, L. J.; Hughes, H. P. *Surf. Sci.* **1995**, *333*, 419.
(32) Pettenkofer, C.; Jaegermann, W.; Schellenberger, A.; Holub-Krappe, E.; Papageorgopoulos, C. A.; Kamaratos, M.; Papageorgopoulos, A. *Solid State Commun.* **1992**, *84*, 921.
(33) Pettenkofer, C.; Jaegermann, W. *Phys. Rev. B* **1994**, *50*, 8816.
(34) Starnberg, H. I.; Brauer, H. E.; Strocov, V. N. *Surf. Sci.* **1997**, *384*, L785.
(35) Crawack, H. J.; Tomm, Y.; Pettenkofer, C. *Surf. Sci.* **2000**, *465*, 301.
(36) Schellenberger, A.; Jaegermann, W.; Pettenkofer, C.; Tomm, Y. *Ionics* **1995**, *1*, 115.
(37) Jaegermann, W.; Pettenkofer, C.; Schellenberger, A.; Papageorgopoulos, C. A.; Kamaratos, M. *Chem. Phys. Lett.* **1994**, *221*, 441.
(38) Hunger, R.; Pettenkofer, C.; Scheer, R. *Surf. Sci.* **2001**, *477*, 76.
(39) Tonti, D.; Pettenkofer, C.; Jaegermann, W. *Ionics* **2000**, *6*, 196.
(40) Yeh, J. J.; Lindau, I. *At. Data Nucl. Data Tables* **1985**, *32*, 1.
(41) Tonti, D.; Pettenkofer, C.; Jaegermann, W. To be published.
(42) Aruga, T.; Murata, T. *Prog. Surf. Sci.* **1989**, *31*, 61.
(43) Nagelberg, A. S.; Worrell, W. L. *J. Solid State Chem.* **1979**, *29*, 345.
(44) Abraham, K. M.; Pitts, L.; Schiff, L. *J. Electrochem. Soc.* **1980**, *127*, 2545.
(45) Zanini, M.; Shaw, J. L.; Tennenhouse, G. J. *J. Electrochem. Soc.* **1981**, *128*, 1647.
(46) Newman, G. H.; Klemann, L. P. *J. Electrochem. Soc.* **1980**, *127*, 2097.
(47) Thompson, A. H.; Symon, C. R.; Gamble, F. R. *Mater. Res. Bull.* **1975**, *10*, 915.
(48) Whittingham, M. S.; Panella, J. A. *Mater. Res. Bull.* **1981**, *16*, 37.